Journal of Alloys and Compounds 489 (2010) 80–83

Contents lists available at ScienceDirect

Journal of Alloys and Compounds

journal homepage: www.elsevier.com/locate/jallcom

New nickel-based bulk metallic glasses with extremely high nickel content

Yuqiao Zeng[a,*], Chunling Qin[b], Nobuyuki Nishiyama[c,1], Akihisa Inoue[a,b,2]

[a] Institute for Materials Research, Tohoku University, 2-1-1 Katahira, Aoba-Ku, Sendai 980-8577, Japan
[b] WPI, Advanced Institute for Materials Research, Tohoku University, Sendai 980-8577, Japan
[c] R&D Institute of Metals and Composites for Future Industries (RIMCOF), Katahira 2-1-1, Aoba-ku, Sendai 980-8577, Japan

ARTICLE INFO

Article history:
Received 8 January 2009
Accepted 6 September 2009
Available online 11 September 2009

Keywords:
Amorphous materials
Rapid-solidification
Quenching

ABSTRACT

The effect of boron addition on glass formation in the $Ni_{70}Pd_{10}P_{20}$ alloy was investigated. The composition containing 4 at% boron showed an improved glass-forming ability. A glassy $Ni_{70}Pd_{10}P_{16}B_4$ alloy rod with a diameter of 2.5 mm was prepared by a copper mold casting technique. This is the first time that a Ni-based bulk metallic glass with such an extremely high Ni content of 70 at% has been produced. The obtained glassy $Ni_{70}Pd_{10}P_{16}B_4$ alloy exhibited rather good mechanical properties and corrosion resistance.

1. Introduction

In the late 1980s, bulk metallic glasses (BMGs) with exceptional glass-forming ability (GFA) and unique physical, mechanical, and chemical properties [1] were developed in various systems such as Al- [2], Mg- [3], Zr- [4,5], and Pd–Cu-based [6] alloys. This important landmark demonstrates that BMGs are not a laboratory curiosity anymore and have potential for practical applications. Therefore, the exploration of BMGs has become one of the hottest topics in material science and engineering.

In the case of Ni-based BMGs, though initialed comparatively as newcomers to BMG family, they are considered as one of the most important BMG systems since these BMGs exhibit ultrahigh strength and outstanding corrosion resistance, favorable for engineering applications. Consequently, great effort has been devoted to develop Ni-based BMGs. Following the first success in the formation of BMG with a diameter of 1 mm in Ni–Nb–Cr–Mo–P–B system [7], several Ni-based BMGs with rather high GFA and large critical diameters for glass formation (d_c) were developed, such as Ni–Nb–Zr–Ti–Co–Cu (d_c = 3 mm) [8], Ni–Ta–Sn (d_c = 2 mm) [9], Ni–Zr–Ti–Nb–Si–Sn (d_c = 5 mm) [10], and Ni–Cu–Ti–Zr–Al–(Si) (d_c = 5 mm) [11] alloys. Most of these BMG compositions contain 45–65 at% nickel, and there have been no report on the formation of Ni-based BMGs with nickel content above 65 at% due to the low GFA of these compositions. Recently, minor boron doping has been found to dramatically improve the GFA of Ni–Pd–P alloys [12]. The d_c of $Ni_{60}Pd_{20}P_{20}$ was enlarged from below 6 mm to higher than 15 mm by the addition of 3 at% boron. In the present study, a Ni-based Ni–Pd–P–B BMG with an extremely high nickel content of 70 at% was developed by the minor boron doping technique. The thermal stability, mechanical properties, and corrosion resistance of the new BMG were investigated and the reasons for the effectiveness and sensitivity of boron addition on GFA and thermal stability were discussed.

2. Experimental

Mother alloys with nominal compositions of $Ni_{70}Pd_{10}P_{20-x}B_x$ ($0 \le x \le 8$) were prepared by melting a mixture of pure nickel and palladium metals, boron crystal and pre-alloyed Pd–Ni–P ingots in vacuumed fused silica tubes, followed by a B_2O_3 flux treatment. Ribbon samples with a cross section of 0.02 mm × 1.2 mm were prepared by a single-roller melt-spinning technique. Cylindrical bulk samples were prepared by copper mold casting. The amorphous nature of the as-prepared samples was characterized by X-ray diffraction (XRD) with $CuK_{\alpha l}$ radiation and by transmission electron microscopy (TEM). The thermal properties were studied with a differential scanning calorimeter (DSC) at a heating rate of 0.67 K/s in a purified argon atmosphere. Mechanical properties were examined using an Instron machine at a strain rate of 5×10^{-4} s^{-1}. The gauge dimensions were 2 mm in diameter and 4 mm in length. Fracture features were observed with a scanning electron microscope (SEM). Electrochemical measurements were conducted in a three-electrode cell using a platinum counter electrode and an Ag/AgCl reference electrode. Potentiodynamic polarization curves were measured at a potential sweep rate of 50 mV min^{-1} after open-circuit immersion for about 20 min when the open-circuit potential had become almost steady.

3. Results and discussion

Fig. 1 shows the DSC curves of the as-spun $Ni_{70}Pd_{10}P_{20-x}B_x$ ribbons prepared by the melt-spinning technique. The alloys containing 0–8 at% boron exhibit an endothermic peak due to glass

* Corresponding author. Tel.: +81 22 215 2112.
E-mail addresses: zyuqiao@imr.tohoku.ac.jp (Y. Zeng), rimcofnn@imr.tohoku.ac.jp (N. Nishiyama), ainoue@imr.tohoku.ac.jp (A. Inoue).
[1] Tel.: +81 22 215 2840.
[2] Tel.: +81 22 215 2111.

0925-8388/$ – see front matter © 2009 Elsevier B.V. All rights reserved.
doi:10.1016/j.jallcom.2009.09.016

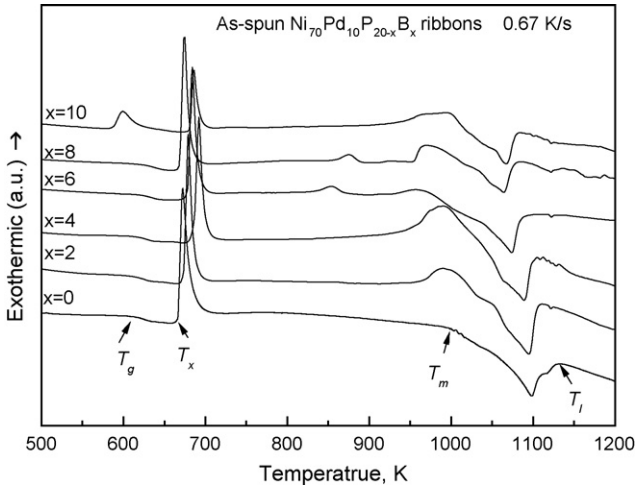

Fig. 1. DSC curves of the as-spun $Ni_{70}Pd_{20}P_{20-x}B_x$ ribbon samples at a heating rate of 0.67 K/s.

Table 1
Thermal analysis data and evaluation parameters for GFA of as-spun $Ni_{70}Pd_{10}P_{20-x}B_x$ ribbons determined by DSC at a scanning rate of 0.67 K/s.

$Ni_{70}Pd_{10}P_{20-x}B_x$	T_g/K	T_x/K	T_m/K	T_l/K	ΔT_x/K	T_{rg}	γ
$x=0$	618	665	988	1132	47	0.546	0.380
$x=2$	619	669	1014	1125	50	0.550	0.384
$x=4$	620	683	1015	1126	63	0.550	0.391
$x=6$	623	678	977	1125	55	0.553	0.388
$x=8$	626	668	1006	1188	42	0.527	0.368
$x=10$	–	585	1008	1183	–	–	–

transition, followed by a supercooled liquid region and then a sharp exothermic peak due to crystallization. With further increasing temperature, the samples are completely melted after several endothermic steps. Table 1 summarizes the thermal analysis data including the onset temperature of glass transition (T_g), crystallization (T_x) and melting (T_m), as well as the finishing temperature of melting (T_l). From these basic thermal data, the quantitative parameters revealing GFA, i.e., ΔT_x (=$T_x - T_g$), T_{rg} (=T_g/T_l), and γ (= $T_x/(T_g + T_l)$), were derived and are listed in Table 1. With increasing boron content, T_g increases slightly from 618 K at $x=0$ to 626 K at $x=8$ and disappears at $x=10$, and T_x first increases from 665 K

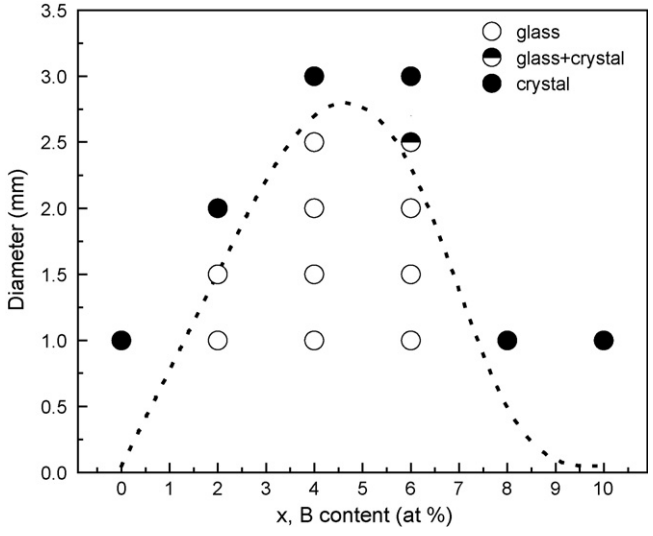

Fig. 2. The d_c of $Ni_{70}Pd_{10}P_{20-x}B_x$ produced by copper mold casting as a function of boron content.

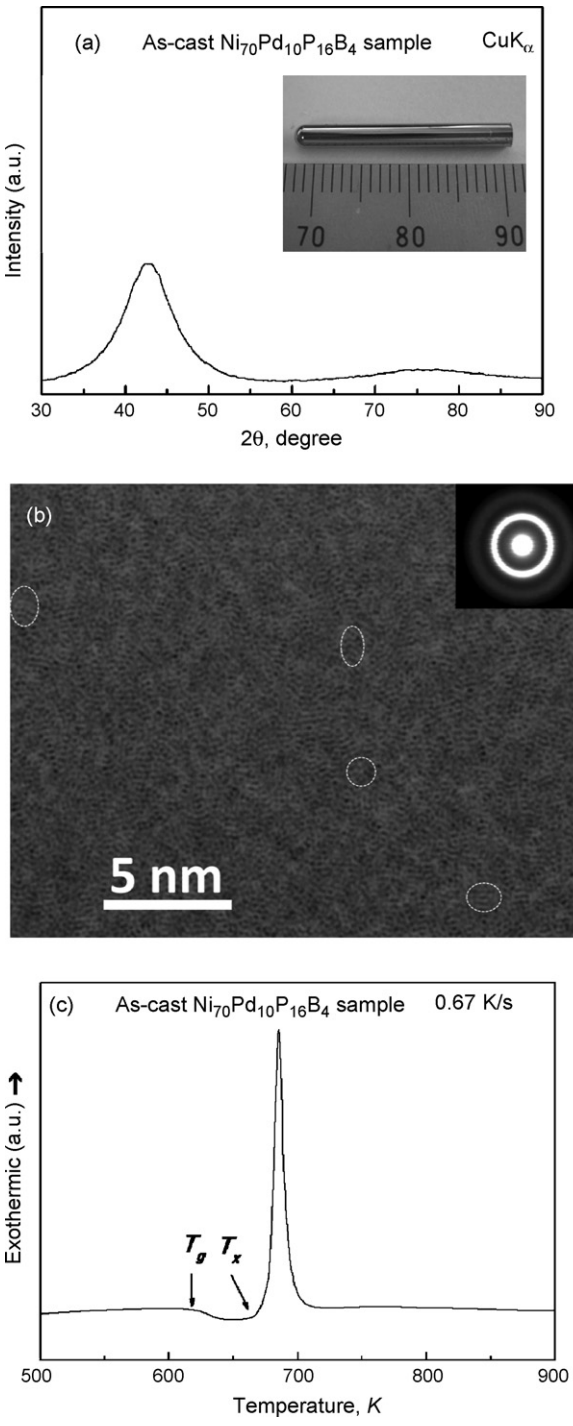

Fig. 3. Formation of a $Ni_{70}Pd_{10}P_{16}B_4$ BMG with a diameter of 2.5 mm. (a) Outer appearance and XRD pattern, (b) high-resolution TEM images and selected area diffraction pattern, and (c) DSC trace of the Ø2.5 mm $Ni_{70}Pd_{10}P_{16}B_4$ samples.

at $x=0$ to 683 K at $x=4$ and then decreases down to 585 K at $x=10$, while T_m and T_l show more complex changing tendency with increasing boron addition. As a result, ΔT_x first increases by a small amount of boron addition, from 47 K at $x=0$ to 63 K at $x=4$, and then significantly decreases down to 42 K at $x=8$. The rather large ΔT_x value (63 K) of the as-spun $Ni_{70}Pd_{20}P_{16}B_4$ ribbon sample indicates the improvement of thermal stability by minor boron addition. The γ and T_{rg} values show the similar composition dependence of ΔT_x, except that the maxim T_{rg} of 0.553 appears at $x=6$, and the maxim γ of 0.391 appears at $x=4$, respectively. The disagreement in the

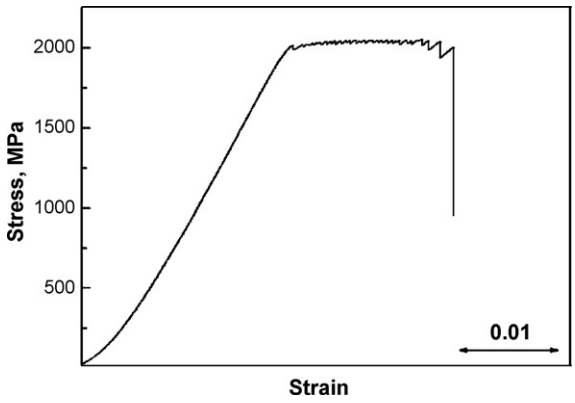

Fig. 4. Nominal compressive stress–strain curve of the $Ni_{70}Pd_{10}P_{16}B_4$ BMG.

optimum boron contents among the parameters is caused by the difference in characteristics of each parameter [13]. However these results suggest that the highest GFA lies in the composition vicinity of $x = 4–6$.

With the aim of confirming the best glass-forming composition in $Ni_{70}Pd_{10}P_{20-x}B_x$, the critical diameter for glass formation (d_c) was investigated for the bulk alloys prepared by copper mold casting, the results being shown in Fig. 2. BMGs with diameters larger than 1 mm in $Ni_{70}Pd_{10}P_{18}B_2$, $Ni_{70}Pd_{10}P_{16}B_4$, and $Ni_{70}Pd_{10}P_{14}B_6$ alloys were produced, the first time that Ni-based BMGs with such extremely high nickel content have ever been obtained by a conventional cooling method. The d_c was 1.5 mm at $x = 2$, 2.5 mm at $x = 4$, and 2.0 mm at $x = 6$, being consistent with the composition dependence of ΔT_x and γ. Clearly, $Ni_{70}Pd_{10}P_{16}B_4$ is the best glass-forming composition as evidenced by its largest d_c of 2.5 mm among $Ni_{70}Pd_{10}P_{20-x}B_x$. The outer appearance of the Ø2.5 mm $Ni_{70}Pd_{10}P_{16}B_4$ sample is shown in the inset of Fig. 3(a). The surface is mirror like lustrous and smooth, and no cavities caused by a crystalline phase are presented. The corresponding XRD spectra of the Ø2.5 mm $Ni_{70}Pd_{10}P_{16}B_4$ sample are shown in Fig. 3(a). There is only a broad diffraction maximum without any observable crystalline peaks, demonstrating the formation of a fully amorphous structure. TEM characterization further confirmed the amorphous nature. As shown in Fig. 3(b), detectable nanocrystallites that may be ignored by XRD are not detected by high-resolution electron microscopy. Fig. 3(c) presents the DSC trace of the Ø2.5 mm $Ni_{70}Pd_{10}P_{16}B_4$ sample, which displays the characteristic glass transition feature of glassy alloys.

Apparently, the minor addition of boron plays an important role in the improvement of thermal stability and GFA of the $Ni_{70}Pd_{10}P_{20}$ alloy. Similar effects of minor element doping have been widely reported in a number of alloy systems and several possible mechanisms, including scavenging harmful impurities, change of liquid behavior, stabilization of the liquid state and suppression of the competing crystallization, have been suggested [14,15]. For the distinctive effect of boron in the GFA of Ni-based Ni–Pd–P, one may consider that boron plays a main role in the reduction of heteronucleates by impurity scavenging. However such a possibility has been disproved by the finding of Li et al. [16]. In their work, even though 10 at% boron was added into the Pd–Ni–P alloy, the XPS experiment did not reveal the presence of any B_2O_3 [16]. The most likely cause for the change of the thermal stability and GFA may come from two aspects, i.e., improved effective atomic packing by the much smaller boron atoms and stronger atomic interaction. The increased mismatch in atomic size makes it possible to produce denser atomic packing, resulting in higher viscosity of the liquid. Moreover, the change of atomic interaction may also contribute to the stronger liquid behavior. Chen has pointed out that the unilateral effect of the mismatch in atomic size results in the increase of the mismatch energy and thereby causes the decrease in T_g [17]. However, the addition of much smaller boron atoms into $Ni_{70}Pd_{10}P_{20}$ leads to higher T_g, as shown in Table 1, indicating that the increase in interatomic bonding strength may not be ignored [17]. The partial substitution of phosphorous by boron may form some stronger chemical bonds which favor the short/medium-range ordering in glass-forming alloys, and stronger local ordering leads to a decrease of the configuration entropy of liquids and thus higher GFA. However, the decrease in GFA with a further addition of boron ($x > 6$) may also be attributed to the strengthened bonding. Once the chemical bonding becomes sufficiently strong, it triggers the formation of intermetallic phases and destabilizes the supercooled liquid, which is evidenced by the decrease in T_x with increasing boron addition.

In industrial application, mechanical properties are important as well as GFA. Therefore the mechanical properties of the $Ni_{70}Pd_{10}P_{16}B_4$ alloy were tested under a compressive load. The nominal stress–strain curve is shown in Fig. 4 where the slope is calibrated by using a strain-gauge setup. The alloy exhibits a rather low Young's modulus of 110 GPa and high strength of 2060 MPa. It should be noted that the BMG also exhibits a distinctive plastic strain of about 0.02. Fig. 5 shows the fracture morphology of $Ni_{70}Pd_{10}P_{16}B_4$ BMG subjected to a compressive fracture. Just as in the case of many other BMGs which exhibit a fracture away from the maximum shear stress plane, the $Ni_{70}Pd_{10}P_{16}B_4$ BMG

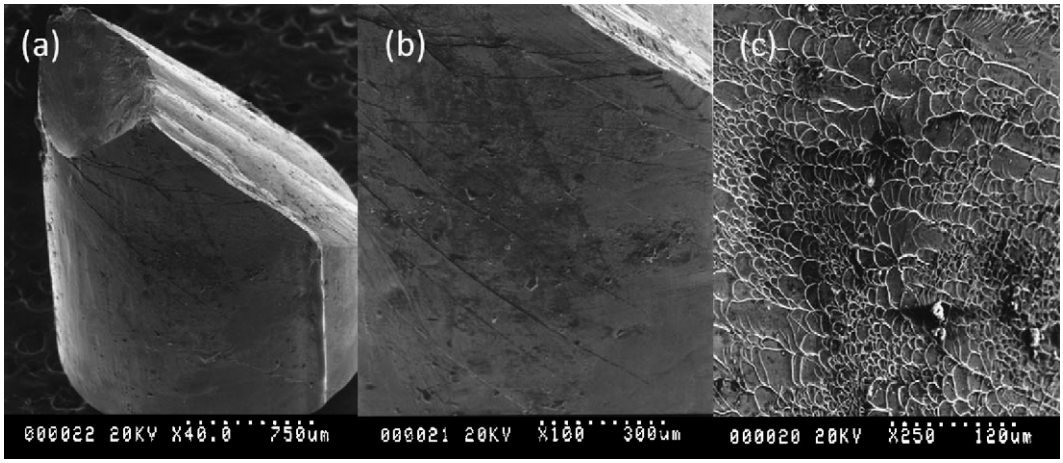

Fig. 5. SEM images of the $Ni_{70}Pd_{10}P_{16}B_4$ BMG subjected to fracture under a compressive load.

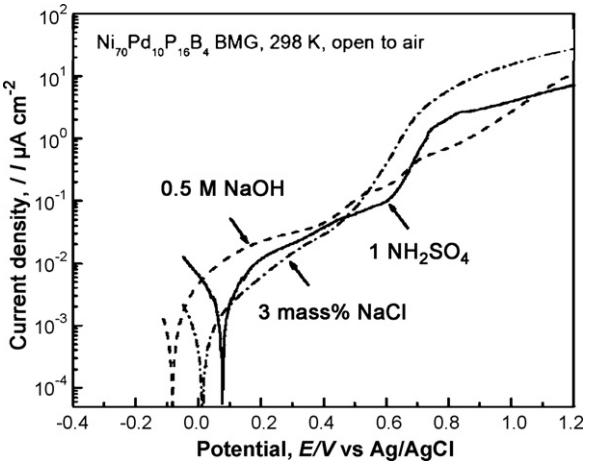

Fig. 6. Anodic polarization curves of the $Ni_{70}Pd_{10}P_{16}B_4$ BMG.

shows a fracture angle of about 41–42° to the compressive loading direction [18–20], indicating that the yield behavior of this BMG follows the Mohr–Coulomb criterion rather than the von Mises criterion [19]. Clear vein-like patterns can be observed on the fracture surface, demonstrating a pure shear fracture process of the $Ni_{70}Pd_{10}P_{16}B_4$ BMG. Instead of a single shear band that leads to a catastrophic failure, multiple shear bands are distributed on the outer surface of the deformed sample. The formations of these multiple shear bands might be caused by the medium-range ordered (MRO) regions dispersed in the glassy matrix, as shown in Fig. 3(b). The stress distribution around the MRO regions can be changed to a three-dimensional stress condition even under a uniaxial load, which is expected to cause the suppression of highly localized shear band propagation through the generation of a multiple shear stress condition.

In order to obtain basic data of use for industrial application, the corrosion behavior was also examined by electrochemical measurements. Fig. 6 shows the anodic polarization curves of the as-cast Ni-based BMG rods with a diameter of 2.5 mm in 1N H_2SO_4, 3 mass% NaCl and 0.5 M NaOH solutions open to air at 298 K. All the Ni-based alloys are spontaneously passivated in these solutions, indicating that the present alloy demonstrates a rather good corrosion resistance in acidic, chloride-ions-containing neutral and alkaline solutions. In addition, the open-circuit potentials of the alloy are about −83.1, 13.2 and 76.9 mV (vs. Ag/AgCl) in NaOH, NaCl and H_2SO_4 solutions, respectively. It is clearly seen that the open-circuit potentials of the alloy are nobler with increasing acidity of the solutions.

4. Conclusions

New Ni-based BMGs with an extremely high Ni content of 70 at% were developed by minor boron doping. The alloy containing 4 at% of boron showed a distinctively improved GFA. A glassy rod with a diameter up to 2.5 mm was obtained by copper mold casting. The $Ni_{70}Pd_{20}P_{16}B_4$ BMG exhibited rather high fracture strength of 2060 MPa with a distinct plastic strain of 0.02 and rather good corrosion resistance in various solutions. The good combination of strength, plasticity and corrosion resistance indicates that this new glassy alloy is a promising candidate for engineering applications.

Acknowledgements

The authors gratefully acknowledge the financial support by the Global Center of Excellence (GCOE). This work was supported (in part) by Global COE Program “Materials Integration (International Center of Education and Research), Tohoku University,” MEXT, Japan.

References

[1] A. Inoue, Acta Mater. 48 (2000) 279–306.
[2] A. Inoue, T. Zhang, T. Masumoto, Mater. Trans. JIM 30 (1989) 965–972.
[3] A. Inoue, H. Kato, T. Zhang, S.G. Kim, T. Masumoto, Mater. Trans. JIM 32 (1991) 609–616.
[4] A. Inoue, T. Zhang, T. Masumoto, Mater. Trans. JIM 31 (1990) 177–183.
[5] A. Peter, W.L. Johnson, Appl. Phys. Lett. 63 (1993) 2342–2344.
[6] A. Inoue, N. Nishiyama, T. Matsuda, Mater. Trans. JIM 37 (1996) 181–184.
[7] X. Wang, I. Yoshii, A. Inoue, Y. Kim, I. Kim, Mater. Trans. JIM 40 (1999) 1130–1136.
[8] T. Zhang, A. Inoue, Mater. Trans. JIM 43 (2002) 708–711.
[9] H.Y. Tien, C.Y. Lin, T.S. Chin, Intermetallics 14 (2006) 1075–1078.
[10] J.Y. Lee, D.H. Bae, J.K. Lee, D.H. Kim, J. Mater. Res. 19 (2004) 2221–2225.
[11] D. Xu, G. Duan, W.L. Johnson, C. Garland, Acta Mater. 52 (2004) 3493–3497.
[12] Y. Zeng, A. Inoue, N. Nishiyama, M.W. Chen, Scripta Mater. 60 (2009) 925–928.
[13] N. Nishiyama, A. Inoue, Mater. Trans. JIM 43 (2002) 1913–1917.
[14] C.T. Liu, Z.P. Lu, Intermetallics 13 (2005) 415–418.
[15] W.H. Wang, Prog. Mater. Sci. 52 (2007) 540–596.
[16] Q. Li, D. Greig, S.H. Kilcoyne, P.J. Hine, J.A.D. Matthew, G. Beamson, Mater. Sci. Eng. A 408 (2005) 154–157.
[17] H. Chen, Rep. Prog. Phys. 43 (1980) 353–432.
[18] W.J. Wright, R. Saha, W.D. Nix, Mater. Trans. JIM 42 (2001) 642–649.
[19] Z.F. Zhang, J. Eckert, L. Schultz, Acta Mater. 51 (2003) 1167–1179.
[20] P.E. Donovan, Acta Metall. 37 (1989) 445–456.